THE FASEB JOURNAL • RESEARCH • www.fasebj.org

GM-CSF– and M-CSF–primed macrophages present similar resolving but distinct inflammatory lipid mediator signatures

Ana Lukic,* Pia Larssen,† Alexander Fauland,* Bengt Samuelsson,* Craig E. Wheelock,* Susanne Gabrielsson,† and Olof Radmark*,[1]

*Division of Physiological Chemistry II, Department of Medical Biochemistry and Biophysics, and †Immunology and Allergy Unit, Department of Medicine Solna, Karolinska Institutet, Stockholm, Sweden

ABSTRACT: M1 and M2 activated macrophages (Mϕs) have different roles in inflammation. Because pathogens may first encounter resting cells, we investigated lipid mediator profiles prior to full activation. Human monocytes were differentiated with granulocyte Mϕ colony-stimulating factor (GM-CSF) or Mϕ colony-stimulating factor (M-CSF), which are known to prime toward M1 or M2 phenotypes, respectively. Lipid mediators released during resting conditions and produced in response to bacterial stimuli (LPS/*N*-formylmethionyl-leucyl-phenylalanine or peptidoglycan) were quantified by liquid chromatography-mass spectrometry. In resting conditions, both Mϕ phenotypes released primarily proresolving lipid mediators (prostaglandin E_2 metabolite, lipoxin A_4, and 18-hydroxyeicosapentaenoic acid). A striking shift toward proinflammatory eicosanoids was observed when the same cells were exposed (30 min) to bacterial stimuli: M-CSF Mϕs produced considerably more 5-lipoxygenase products, particularly leukotriene C_4, potentially linked to M2 functions in asthma. Prostaglandins were formed by both Mϕ types. In the M-CSF cells, there was also an enhanced release of arachidonic acid and activation of cytosolic phospholipase A_2. However, GM-CSF cells expressed higher levels of 5-lipoxygenase and 5-lipoxygenase–activating protein, and in ionophore incubations these cells also produced the highest levels of 5-hydroxyeicosatetraenoic acid. In summary, GM-CSF and M-CSF Mϕs displayed similar proresolving lipid mediator formation in resting conditions but shifted toward different proinflammatory eicosanoids upon bacterial stimuli. This demonstrates that preference for specific eicosanoid pathways is primed by CSFs before full M1/M2 activation.—Lukic, A., Larssen, P., Fauland, A., Samuelsson, B., Wheelock, C. E., Gabrielsson, S., Radmark, O. GM-CSF– and M-CSF–primed macrophages present similar resolving but distinct inflammatory lipid mediator signatures. FASEB J. 31, 4370–4381 (2017). www.fasebj.org

KEY WORDS: eicosanoid · M1 · M2 · leukotriene · lipoxin

Macrophages (Mϕs) orchestrate the inflammatory process from early onset to the resolution phase (1, 2). A major issue in Mϕ biology is to characterize functional phenotypes, currently described as a heterogeneous spectrum of activated states, from M1 to M2 (3, 4). Stimulating factors, such as cytokines and pathogens, can induce specific phenotypes: originally IFN-γ + LPS activation resulted in a proinflammatory M1 state, whereas IL-4 activation induced the alternatively activated M2 state. Polarized cells express distinct markers, such as transcription factors, cytokines, and surface markers; these are the main tools to define Mϕ phenotypes. A number of transcripts have been reported to differ between M1 and M2 Mϕs, including mRNAs for enzymes involved in eicosanoid metabolism (5).

Eicosanoids originate from arachidonic acid (AA), released from membrane phospholipids by phospholipases, typically cytosolic phospholipase A_2 ($cPLA_2$) (6). Free AA is further metabolized *via* 3 enzymatic pathways: lipoxygenase (LO), cyclooxygenase (COX), and cytochrome P450 (CYP), leading to leukotrienes (LTs), hydroxyeicosatetraenoic acids (HETEs), prostaglandins (PGs), and epoxyeicosatrienoic acids (EpETrEs). By transcellular pathways AA can be converted to proresolving lipoxins (LXs), generated *via* 15-LO-1 and 5-LO or by 5-LO and

ABBREVIATIONS: AA, arachidonic acid; CLP, coactosin-like protein; COX, cyclooxygenase; $cPLA_2$, cytosolic phospholipase A_2; CYP, cytochrome P450; Cys-LT, cysteinyl leukotriene; EPA, eicosapentaenoic acid; EpETrE, epoxyeicosatrienoic acid; FLAP, 5-lipoxygenase activating protein; fMLP, *N*-formylmethionyl-leucyl-phenylalanine; GM-CSF, granulocyte macrophage colony-stimulating factor; HEPE, hydroxyeicosapentaenoic acid; HETE, hydroxyeicosatetraenoic acid; LC-MS/MS, liquid chromatography-tandem mass spectrometry; LO, lipoxygenase; LT, leukotriene; LX, lipoxin; Mϕ, macrophage; M-CSF, macrophage colony-stimulating factor; mPGES, microsomal prostaglandin E synthase; P-$cPLA_2$, phosphorylated $cPLA_2$; PGEM, prostaglandin E_2 metablolite; PGN, peptidoglycan; pp, positive pressure; RvE, resolvin E; SPE, solid-phase extraction; Tx, thromboxane

[1] Correspondence: Division of Physiological Chemistry II, Department of Medical Biochemistry and Biophysics, Karolinska Institutet, Scheeles väg 2, SE-171 77, Stockholm, Sweden. E-mail: olof.radmark@ki.se

doi: 10.1096/fj.201700319R

This article includes supplemental data. Please visit *http://www.fasebj.org* to obtain this information.

0892-6638/17/0031-4370 © FASEB

12-LO (7). Recently it was reported that LXA_4 and 15-epi-LXA_4 could also be formed within one cell type (murine RAW264.7 and bone marrow–derived Mϕs) (8). Depending on the expression and activation of eicosanoid-forming enzymes and their proximity to $cPLA_2$, cells may preferentially shunt AA toward one of these pathways (6). Lipidomic analysis has been applied to study AA metabolism in mouse peritoneal Mϕs (9), RAW264.7 Mϕs (10, 11), mouse mast cells (12), and Mϕs from mouse lung tumors (13). Lipid mediators released from fully activated M1 and M2 human Mϕs have also been determined (14).

Fully activated M1/M2 Mϕs may be considered as endpoints of the corresponding activation (or differentiation) schemes. However, Mϕ differentiation leads to a diverse spectrum of cell types (4). Here we aimed to determine eicosanoid production in Mϕ phenotypes before their full activation because this is likely the state of the cell when pathogens are encountered. We therefore used cells differentiated with only granulocyte Mϕ colony-stimulating factor (GM-CSF) or Mϕ colony-stimulating factor (M-CSF), which have been described to prime Mϕs toward M1 and M2 phenotypes, respectively, but not to the fully activated states (15). Lipid mediators released spontaneously to the cell culture medium during 24 h or produced in response to bacterial alarm signals with 30-min incubations with LPS/*N*-formylmethionyl-leucyl-phenylalanine (fMLP) and peptidoglycan (PGN) were analyzed by liquid chromatography-tandem mass spectrometry (LC-MS/MS). We found that the two Mϕ types released mainly proresolving lipid mediators in resting conditions, suggesting that both phenotypes could support maintenance of tissue homeostasis in the steady state. Upon bacterial stimulation, both Mϕ types promptly shifted toward inflammatory eicosanoids, but with different profiles.

MATERIALS AND METHODS

All materials were purchased from Sigma-Aldrich (St. Louis, MO, USA) unless otherwise stated.

Cell preparation and differentiation

GM-CSF– and M-CSF–differentiated Mϕs were prepared from primary monocytes isolated from buffy coats of healthy human donors (Karolinska Hospital Blood Bank). Peripheral blood mononuclear cells were isolated by gradient centrifugation with Ficoll-Paque Premium (GE Healthcare, Uppsala, Sweden) and seeded at 5×10^6 cells/ml for 2 h, allowing monocytes to adhere to plastic cell culture plates. Cells were then vigorously washed twice with PBS to remove lymphocytes. Finally, monocytes were differentiated for 7 d in RPMI 1640 medium supplemented with glutamine, 10% fetal bovine serum, 100 mg/ml streptomycin, 100 U/ml penicillin, 1× nonessential amino acids, and 25 mM HEPES. Recombinant human GM-CSF (10 ng/ml) or recombinant human M-CSF (10 ng/ml) was added. Cells were supplied with fresh medium and cytokines on d 3 and 6. All analyses were performed with cells and medium collected on d 7.

Phenotypic characterization of Mϕs by ELISA and flow cytometry

Cell culture medium collected after the last 24 h of differentiation (d 7) was analyzed for IL-6 and -10 by ELISA (Mabtech, Stockholm, Sweden). Cells were also phenotyped by flow cytometry as described by Esser *et al*. (16). Cells were stained using the following markers: FITC-labeled anti–HLA-DR, DC-SIGN, CD80 (BioLegend, San Diego, CA, USA); CD14, TLR-2 (BD Biosciences, San Diego, CA, USA); PE-labeled anti CD54 (BioLegend); CD86 (BD Biosciences); and the corresponding isotype controls. Phenotypes were analyzed by FACS Canto (BD Biosciences) and FlowJo software (Tree Star, Ashland, OR, USA).

Incubations with bacterial stimuli

Incubations were performed with adherent GM-CSF and M-CSF Mϕs. After 7 d, medium was replaced by 2 ml/flask PBS containing 1 mg/ml glucose and 1 mM $CaCl_2$. Cells ($1.1–1.8 \times 10^6$) in 2 ml were stimulated with LPS (1 μg/ml) for 20 min followed by fMLP (1 μM) for 10 min. Alternatively, cells were stimulated with PGN (100 μg/ml) for 30 min. Reactions were stopped by 2 ml ice-cold methanol. Cell remains were scraped to collect the entire incubates and stored at −80°C until extraction, and LC-MS/MS analysis was performed. For each donor, an additional flask per phenotype was prepared for cell counting on d 7. Mϕs were also incubated with 40 μM arachidonic acid together with 5 μM A23187 for 10 min at 37°C in 1 ml PBS containing 1 mg/ml glucose and 1mM $CaCl_2$. The reaction was stopped by adding 1 ml of methanol with internal standards.

Lipid mediator analysis by LC-MS/MS

A previously published stable isotope dilution LC-MS/MS method was used for lipid mediator quantification (17), with slight modification to include the cysteinyl leukotrienes (Cys-LTs) LTC_4, LTD_4, and LTE_4. Aliquots of conditioned cell culture medium (1 ml) or stopped cell incubates (0.5 ml) were centrifuged at 10,000 *g* for 10 min at 4°C. To the supernatants, 1.5 or 2 ml of citrate/phosphate buffer (0.1 and 0.2 mM, pH 5.6), respectively, were added, and solutions were spiked with an internal standard mixture. The calibration levels and internal standards are provided in Balgoma *et al*. (17), except for the Cys-LTs (Supplemental Table 2). Lipid mediators were extracted using 3 ml/60 mg Evolute Express ABN solid-phase extraction (SPE) cartridges (Biotage, Uppsala, Sweden) on an Extrahera sample handling system (Biotage). SPE columns were conditioned with 2.5 ml methanol (N_2 positive pressure [pp], 1.3 bars for 90 s) and equilibrated with 2.5 ml water (N_2 pp, 1.5 bars for 90 s). Samples were loaded onto the SPE cartridges (N_2 pp, 1.5 bars for 180 s followed by 3 bars for 30 s). Cell samples were washed with 2 ml of water and cell supernatant samples with 2 ml of water/methanol (80:20, v/v) (N_2 pp, 1.5 bars for 120 s). Then cartridges were dried using a N_2 pp gradient (1.2 bars for 120 s followed by 5 bars for 750 s). Lipids were eluted with 2.5 ml of methanol (N_2 pp, 1 bar for 250 s followed by 5 bars for 150 s). Eluates were evaporated in a gentle stream of N_2 gas until dryness onto an automated TurboVap LV evaporation system (Biotage). Extracts were reconstituted in 70 μl of methanol/water (6:1, v/v) and filtered by centrifugation using 0.1 μm membrane spin filters (Merck Millipore, Billerica, MA, USA). Samples were then transferred to autosampler vials for LC-MS/MS analysis. LC-MS/MS separation and quantification were performed on an UPLC Acquity-Xevo TQ-S mass spectrometer system (Waters, Milford, MA, USA). The autosampler and column were kept at 5 and 60°C, respectively. The injection volume was set to 7.5 μl. Separation was achieved with an Acquity UPLC BEH C18 (2.1 × 150 mm, 1.7 μm) (Waters). Chromatographic and MS conditions were used as previously described (17). For quantification of the CysLTs, a second injection of each sample was performed in positive electrospray ionization mode with the following chromatographic conditions: solvents A (water with 0.2% of formic acid) and B (acetonitrile/isopropanol 90:10, v/v + 0.2% formic acid) at a flow

of 0.45 ml/min. The gradient was initiated with 60% of solvent A, which was decreased linearly to 50% at 4.25 min and to 5% at 4.5 min. The column was then washed with 95% of solvent B for 3 min and equilibrated to initial conditions. Detailed multiple reaction monitoring transitions and chromatographic retention times are reported in Balgoma *et al*. (17), except for the Cys-LTs (Supplemental Table 3).

Analysis of LTs and 5-HETE by HPLC UV detection

Cell incubations to be analyzed by HPLC ultraviolet detection were stopped by the addition of 1 ml of methanol containing internal standards (150 pM PGB_2 and 150 pM 17-OH-C22:4; kind gifts from M. Hamberg, Karolinska Institutet) and kept at −20°C for at least 1 h before extraction. Samples were centrifuged at 10,000 *g* for 10 min at 4°C, and supernatants (~2 ml) were mixed with 2 ml citrate/phosphate buffer pH 5.6. SPE on C18 and HPLC ultraviolet detection were performed as described by Lukic *et al*. (18).

SDS-PAGE and Western blotting

Western blot was performed as described by Esser *et al*. (16). After transfer, nitrocellulose membranes (GE Healthcare) were analyzed with the following antibodies: in-house purified rabbit polyclonal against 5-lipoxygenase (5-LO, 1:500 dilution), 5-LO activating protein (FLAP) (1:300), LTA_4 hydrolase (1:700), LTC_4 synthase (1:300), 15-LO (1:500), and in-house purified chicken polyclonal against coactosin-like protein (CLP, 1:500). Mouse monoclonal antibody against γ-glutamyl transpeptidase 1 (GGT1, 1:500) was from Santa Cruz Biotechnology (Santa Cruz, CA, USA). Rabbit polyclonal antibody for $cPLA_2$ and phosphorylated $cPLA_2$ (P-$cPLA_2$; both used at 1:1000) were from Cell Signaling Technology (Danvers, MA, USA). Rabbit polyclonal antibody against thromboxane (Tx)A synthase (1:1000), COX1 (1:500), and microsomal prostaglandin E synthase (mPGES)1 and -2 (mPGES1, 1:200; mPGES2, 1:500) were purchased from Cayman (Ann Arbor, MI, USA). A peroxidase-conjugated primary antibody against β-actin (1:2000 dilution) and peroxidase-conjugated secondary antibodies (1:2000−1:4000) were from Sigma. Protein bands were detected by enhanced chemiluminescence with a Li-Cor scanner (Lincoln, NE, USA). After scanning, band intensity was calculated with Odyssey Imaging software (Li-Cor).

Data analysis

Statistical analysis was performed with GraphPad Prism 5 software (GraphPad Software, La Jolla, CA, USA). Groups were compared with paired Student's *t* test and 1-way ANOVA, Bonferroni, or Dunn correction. Values of $P < 0.05$ were considered statistically significant.

RESULTS

GM-CSF and M-CSF lead to distinct Mϕ phenotypes

We analyzed markers commonly associated with the M1 and M2 states (15). First, we measured IL-6 and -10 in cell culture medium from the final 24 h of differentiation. GM-CSF Mϕs released higher amounts of proinflammatory IL-6, whereas anti-inflammatory IL-10 release was higher in M-CSF Mϕs (**Fig. 1*A***). Next, we observed that CD86 and ICAM-1, cell surface markers commonly associated with inflammation, were higher in GM-CSF cells (Fig. 1*B*). For HLA-DR and DC-SIGN, the mean fluorescence intensity ratios were similar for the two phenotypes. In comparison, for fully activated M1 cells (GM-CSF with addition of LPS and IFN-γ final 24 h), the relative increments of CD86 and ICAM-1 were more prominent, and HLA-DR and CD80 were up-regulated. Fully activated M2 cells (M-CSF with addition of IL-4 final 24 h) displayed increased DC-SIGN (data not shown). These observations support that the Mϕs obtained with only GM-CSF or M-CSF were not fully activated but were differentiated toward M1 or M2 states, respectively. We also studied surface markers involved in LPS- and PGN-mediated signaling pathways. CD14, which is required for responses to LPS mediated by TLR4 and which may enhance responses to PGN mediated by TLR2 (19), was higher in M-CSF cells, as observed before for M2 (5). The mean fluorescence intensity ratio for TLR2, mediating PGN effects, was comparable between the 2 cell types (Fig. 1*B*). However, M-CSF Mϕs were characterized by a higher percentage of TLR2-positive cells (data not shown). Overall, the results support that GM-CSF and M-CSF induced differentiation of monocytes toward the M1 and M2 endpoints, without fully reaching these endpoints.

Basal and induced formation of lipid mediators in GM-CSF and M-CSF Mϕs

Lipid mediator formation was analyzed by LC-MS/MS in two types of samples. Basal release of mediators was determined by extraction of the conditioned cell culture medium present during the final 24 h of differentiation. Induced formation of eicosanoids was determined by incubating the differentiated washed Mϕs with bacterial stimuli. These were LPS/fMLP (LPS is a TLR4 agonist of Gram-negative bacteria) or PGN for 30 min (PGN is a TLR2 agonist of Gram-positive bacteria).

Basal lipid mediator formation

The most abundant AA-derived eicosanoids found in the conditioned medium were the PGE_2 metabolite tetranor-PGEM and LXA_4 (**Fig. 2*A, B***), whereas essentially no LTs were observed in the conditioned medium (Supplemental Table 1). Similar amounts of tetranor-PGEM were released from both cell types, whereas M-CSF Mϕs produced ~50% more LXA_4 compared with GM-CSF cells. The identity of LXA_4 was confirmed by MS/MS analysis (*m/z* 351, 271, 217, 115) (Supplemental Fig. 1), and LXA_4 was ~10-fold higher in conditioned medium compared with plain medium controls. TxB_2 was in the same range as for LXA_4, with 50% more secreted from M-CSF cells (Fig. 2*C*). Resting GM-CSF Mϕs released more CYP-derived metabolites in comparison to M-CSF Mϕs. The epoxides 11 (12)-EpETrE and 14 (15)-EpETrE were detected (Fig. 2*D*, *E*), as well as the corresponding vicinal diols (Fig. 2*F*, *G*).

The eicosapentaenoic acid (EPA) metabolite 18-HEPE, an intermediate in resolvin E (RvE) formation (20), was more abundant in medium from M-CSF cells (Fig. 2*H*) (20). 14,15-DiHETE, a CYP product of EPA, showed the opposite trend (Fig. 2*I*). 17,18-DiHETE, which has recently been associated with outcomes in patients with implantable cardioverter defibrillators (21), was equally high in medium from both Mϕ types (Fig. 2*J*). M-CSF Mϕs

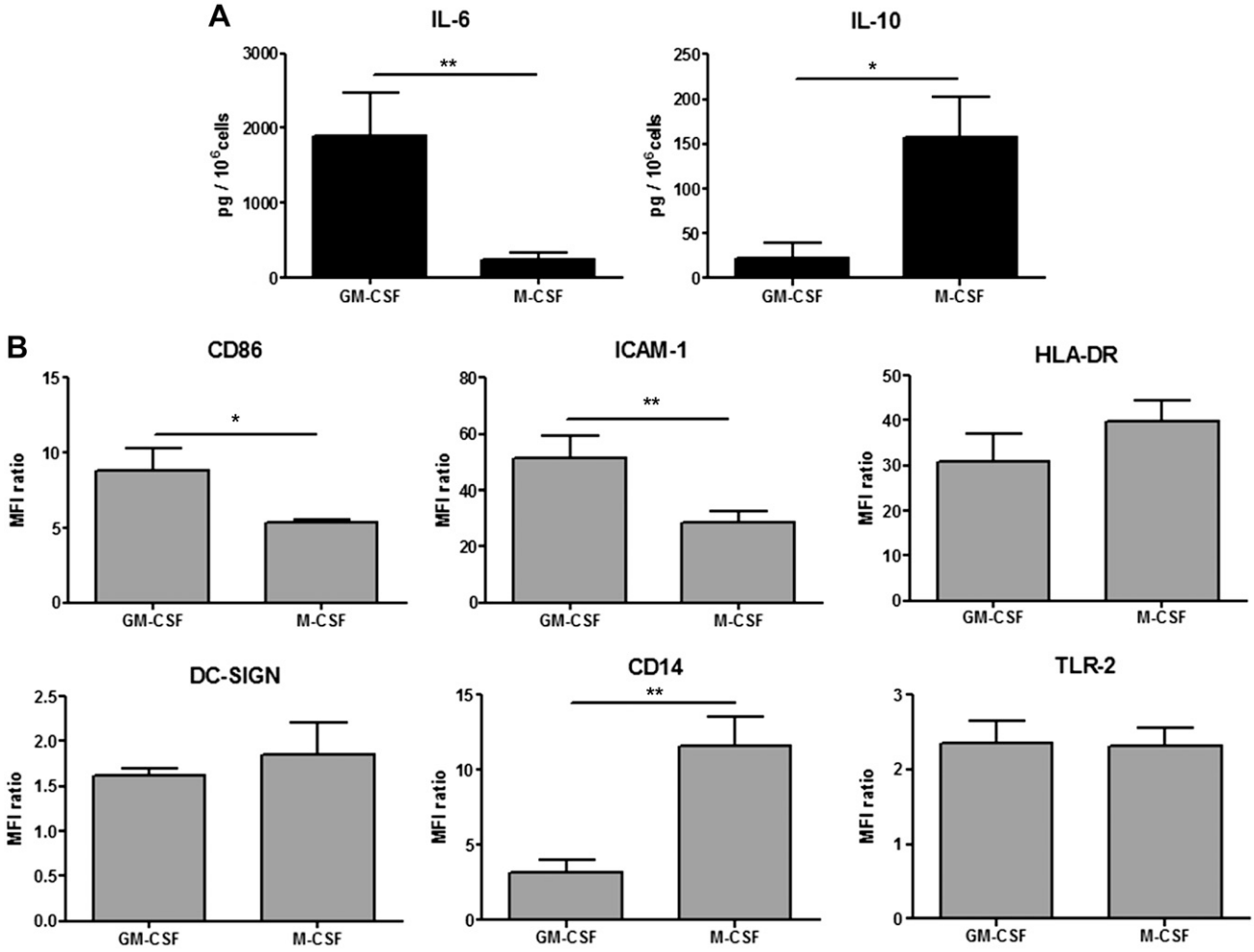

Figure 1. GM-CSF and M-CSF prime differentiation of Mϕs toward M1 and M2 phenotypes. Mϕs were differentiated from human monocytes in the presence of GM-CSF (10 ng/ml) or M-CSF (10 ng/ml) for 7 d. Cytokine release and surface markers associated with the M1 and M2 states were analyzed by ELISA (*A*) and flow cytometry (*B*). Data are presented as means ± SE. ELISA data are based on 6 donors. Flow cytometry data are based on 7 donors for all markers except TLR2 ($n = 5$). Values of $P < 0.05$ were considered significant. $^*P < 0.05$, $^{**}P < 0.01$.

released twice the amount of docosahexaenoic acid–derived 8-hydroxy docosahexaenoic acid, a potential marker of oxidative stress (Fig. 2*K*). 9-KODE was the most abundant linoleic acid metabolite found in cell culture medium, followed by 9,10,13-Tri-HOME (Fig. 2*L*).

Bacterial stimuli induce different eicosanoids

The same GM-CSF and M-CSF Mϕs were incubated with LPS followed by fMLP or with peptidoglycan for 30 min. Regarding AA metabolites, LTB_4 was formed in similar amounts in both GM-CSF–derived and M-CSF–derived cells. LPS/fMLP was the more efficient stimulus compared with peptidoglycan (**Fig. 3*A***). LTC_4 was the clearly dominant LT in incubations of M-CSF Mϕs, and the average level was more than 10-fold higher compared with GM-CSF Mϕs. The capacity for Cys-LT formation varied considerably between donors, but the levels were consistently lower in GM-CSF cells. Considering the role of Cys-LTs in T-helper 2–driven asthma, it is of interest that M2 Mϕs have been emphasized in allergic asthma and inflammation (22). The levels of LTD_4 were 7–15% of LTC_4 (Supplemental Table 1), confirming that LTC_4 metabolism is inefficient in short-time incubations of monocytic cells (18). Also in GM-CSF Mϕs, further conversion to LTD_4 was low, although cells showed a clear glutamyl transpeptidase 1 Western blot band (**Fig. 4**).

5-HETE was the dominant monohydroxy acid formed in the Mϕ incubations, being about 5-fold higher than 12-HETE (incubations with LPS/fMLP) and about 20-fold more compared with 15-HETE (Fig. 3*C–E* and Supplemental Table 1). 5-HETE followed the same pattern as LTC_4 (*i.e.*, it was most abundant in M-CSF–derived cells incubated with LPS/fMLP). LXA_4, which was a major eicosanoid released into the cell culture medium, was a minor product in these 30-min cell incubations (Fig. 3*F*). Among COX products (Fig. 3*G–K*) in the incubations with bacterial stimuli, TxB_2 and 12-hydroxyheptadecatrenoic acid (a side product in thromboxane biosynthesis) dominated, with similar amounts formed in both GM-CSF and M-CSF Mϕs. Also, PGD_2 was produced, particularly in incubations of GM-CSF cells with LPS/fMLP. Less PGE_2 appeared in the incubations, although PGEM was abundant in the conditioned cell culture medium. As a group, CYP

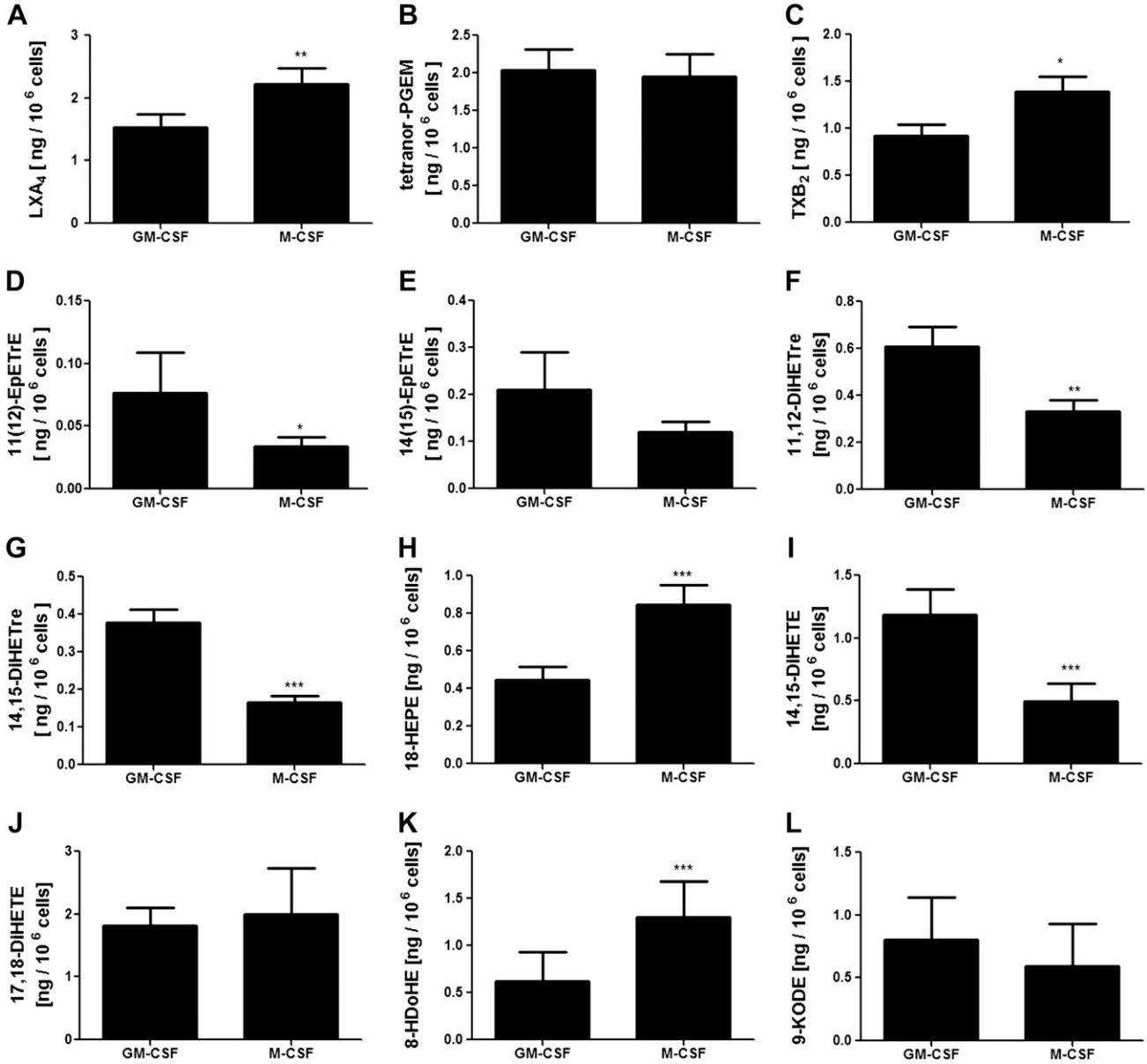

Figure 2. Basal formation and release of lipid mediators from resting GM-CSF– and M-CSF–differentiated Mϕs were determined by analysis of conditioned cell culture medium from the final 24 h of the 7-d differentiation period. Cell culture medium was collected on d 7, and 1 ml of medium (corresponding to ~200,000 cells) was extracted and analyzed by LC-MS/MS. Amounts (ng/10^6 cells) of metabolites LXA_4 (*A*), tetranor-PGEM (*B*), TxB_2 (*C*), 11(12)-EpETrE (*D*), 14(15)-EpETrE (*E*), 11,12-DiHETrE (*F*), 14,15-DiHETrE (*G*), 18-HEPE (*H*), 14,15-DiHETE (*I*), 17,18-DiHETE (*J*), 8-hydroxy docosahexaenoic acid (8-HDoHE) (*K*), and 9-KODE (*L*) are shown. Data are presented as means ± SE of 16 separate cell cultures, 8 donors, and 2 cultures of each cell type from each donor ($n = 16$). $^*P < 0.05$, $^{**}P < 0.01$, $^{***}P < 0.001$.

products were the least abundant eicosanoids formed. However, a striking difference between the 2 Mϕ phenotypes was observed for 5,6-EpETrE, which was 5–6 times higher in incubations of M-CSF cells (Fig. 3*L*). The vicinal diols 11,12-DiHETrE and 14,15-DiHETrE were recovered in all conditions (Supplemental Table 1) but in considerably lower amounts compared with the cell culture medium (Fig. 2).

In incubations with bacterial stimuli, M-CSF Mϕs produced higher amounts of EPA-derived 5-HEPE in comparison to GM-CSF Mϕs and more prominently upon LPS/fMLP (Fig. 3*M*). This was similar as for 5-HETE (Fig. 3*C*); both are 5-LO products. Another abundant EPA-derived metabolite was TxB_3, which was formed in similar amounts in GM-CSF and M-CSF Mϕs (Fig. 3*N*), as observed also for TxB_2 (Fig. 3*G*). Among docosahexaenoic acid–derived products, the RvD intermediate 17-hydroxy docosahexaenoic acid was most abundant, being 1.5 times higher in M-CSF Mϕs with both bacterial stimuli (Fig. 3*O*). The most abundant linoleic acid metabolite was 13-HODE, which was formed in similar amounts in both Mϕ types (Supplemental Table 1).

Expression of eicosanoid-forming enzymes is different in GM-CSF and M-CSF Mϕs

In Western blots, several enzymes for LT biosynthesis, including $cPLA_2$, 5-LO, and FLAP, were expressed to

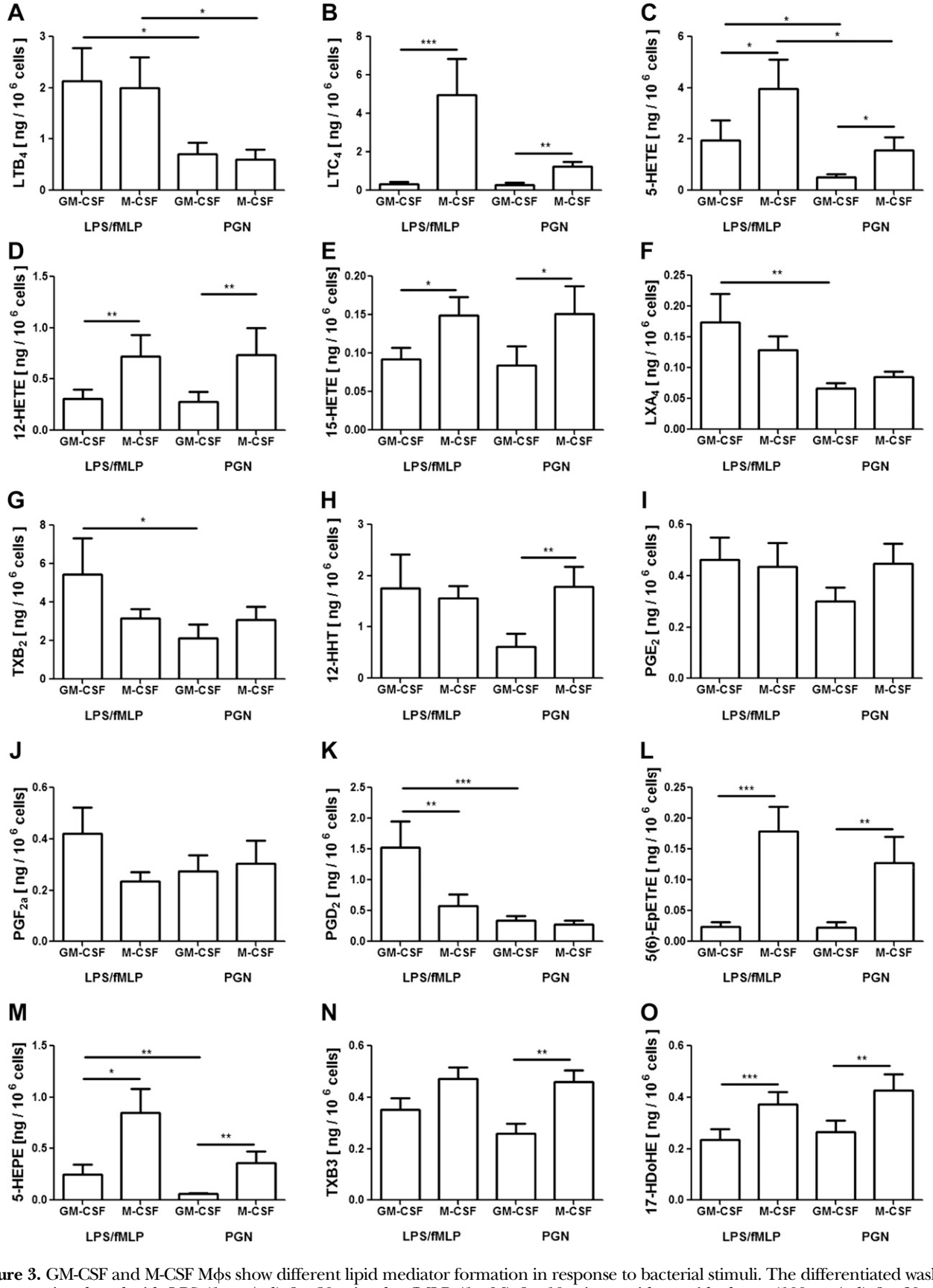

Figure 3. GM-CSF and M-CSF Mϕs show different lipid mediator formation in response to bacterial stimuli. The differentiated washed Mϕs were incubated with LPS (1 μg/ml) for 20 min plus fMLP (1 μM) for 10 min or with peptidoglycan (100 μg/ml) for 30 min. Incubations were stopped with MeOH and extracted, and samples were analyzed by LC-MS/MS. Amounts (pg/10^6 cells) of metabolites LTB_4 (*A*), LTC_4 (*B*), 5-HETE (*C*), 12-HETE (*D*), 15-HETE (*E*), LxA_4 (*F*), TxB_2 (*G*), 12-HHT (*H*), PGE_2 (*I*), PGF_{2a} (*J*), PGD_2 (*K*), 5(6)-EpETrE (*L*), 5-HEPE (*M*), TxB_3 (*N*), and 17-HDoHE (*O*) are shown. For each condition, data are presented as means ± SE of 16 separate incubations, 8 donors, and 2 incubations for each condition ($n = 16$). $^*P < 0.05$, $^{**}P < 0.01$, $^{***}P < 0.001$.

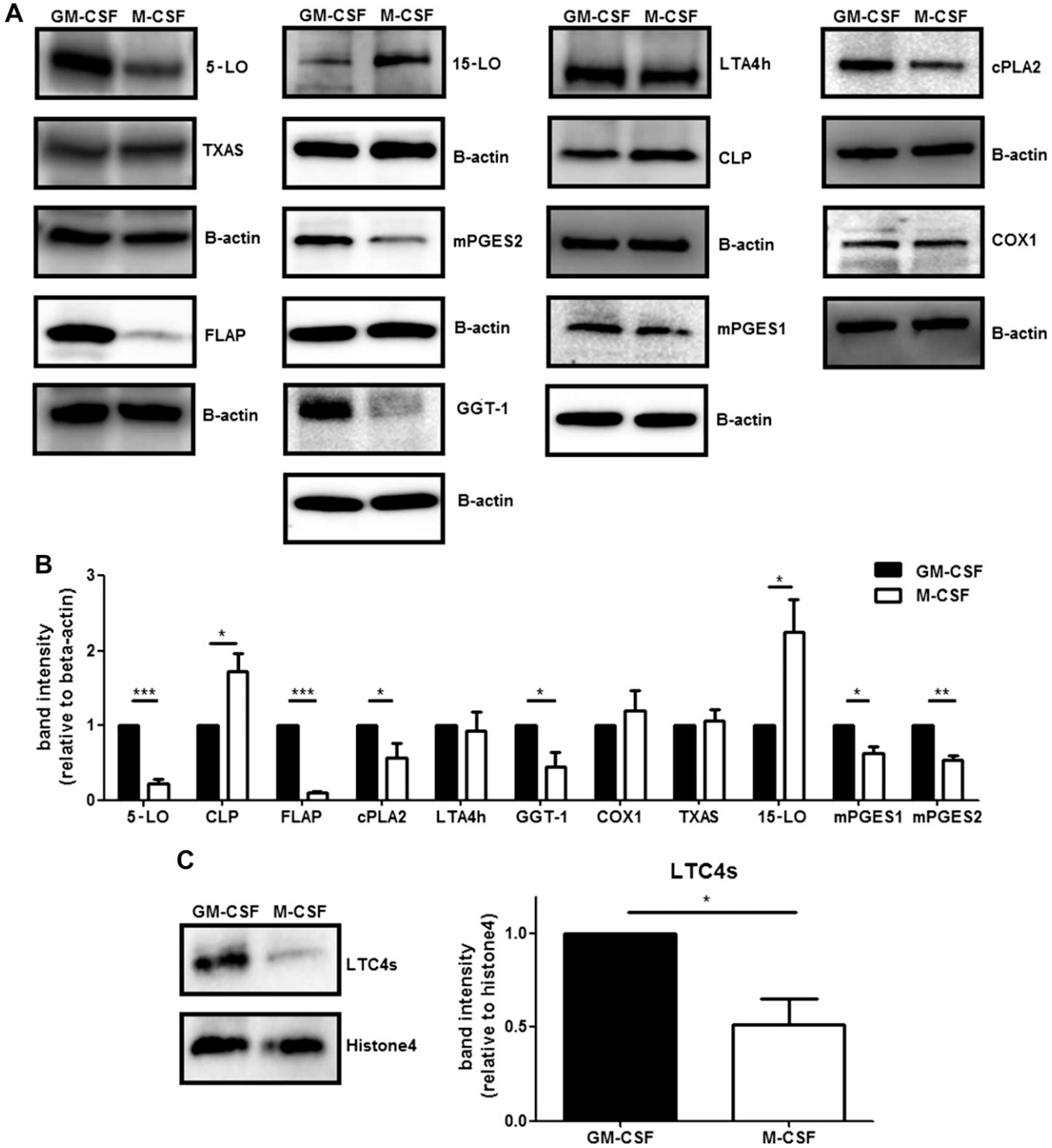

Figure 4. Protein expression of eicosanoid-forming enzymes differs between GM-CSF and M-CSF Mϕs. Cell lysates of unstimulated Mϕs differentiated with GM-CSF (10 ng/ml) or M-CSF (10 ng/ml were prepared on d 7. Protein samples (~40 μg) were analyzed by Western blot for specific eicosanoid-forming enzymes. *A*) Representative blots for each protein. Similar results were observed for 6–9 donors. *B*) Band intensity for each protein was normalized to the corresponding β-actin band, and M-CSF Mϕ values (open bars) were normalized to GM-CSF Mϕ values (black bars). (*C*) Nuclear fractions were prepared after NP-40 lysis (18). LTC_4 synthase band intensities were normalized to Histone4 (nuclear marker), n=4. Data are presented as means ± SE (n = 6–9). $^*P < 0.05$; $^{**}P < 0.01$; $^{***}P < 0.001$.

higher levels in GM-CSF Mϕs compared with M-CSF cells (Fig. 4*A*, *B*). The literature on 5-LO in M1 and M2 Mϕs is controversial. Higher 5-LO and FLAP protein expression has been reported for M1 (23), whereas other reports showed that ALOX5 mRNA was higher in M2 compared with M1 (5, 24). CLP, the other 5-LO accessory protein that also binds to F-actin, was slightly higher in M-CSF Mϕs, whereas LTA_4 hydrolase was equally expressed in both cell types. IL-4–inducible 15-LO (ALOX15) has been included as phenotypical marker for M2 differentiation (3), and our M-CSF Mϕs expressed higher levels of 15-LO protein, in line with M2 transcriptome reports (5, 24).

LTC_4 synthase was determined in nuclear fractions prepared from Mϕs. For the LTC_4 synthase monomer (17 kDa), the protein level was about 2-fold higher in GM-CSF cells compared with M-CSF cells (Fig. 4*C*). As observed previously (16), bands at higher molecular weight were observed, compatible with the presence of LTC_4 synthase dimers and trimers (data not shown). This may reflect the homotrimeric crystal structure of LTC_4 synthase (25). Also, in leukocytes LTC_4 synthase can form complexes with FLAP (26).

We found similar COX-1 protein expression in the GM-CSF and M-CSF Mϕs, whereas COX-2, which is induced in Mϕs during inflammation (6), was not detectable. In previous transcriptome analyses of fully activated M1/M2 cells, COX-1 mRNA was higher in M2, whereas COX-2 dominated in M1 (5, 24). TxA synthase protein expression was comparable in GM-CSF and M-CSF Mϕs, whereas both mPGES-1 and mPGES-2 were higher in GM-CSF cells.

Prompt activation of $cPLA_2$ in M-CSF Mϕs leads to high release of AA

The metabolite data on PG formation in the incubations with LPS/fMLP or peptidoglycan correspond with relative enzyme abundance, whereas this was not the case for the 5-LO pathway. M-CSF Mϕs produced more 5-LO–derived metabolites when stimulated with bacterial agonists in comparison to GM-CSF Mϕs (Fig. 3). This contrasted with the expression of $cPLA_2$, 5-LO, FLAP, and LTC_4 synthase, which was higher in GM-CSF Mϕs (Fig. 4). In the incubations with bacterial stimuli, eicosanoids were produced from endogenous substrate, and, in agreement with the higher 5-LO product formation, M-CSF Mϕs released more AA compared with GM-CSF Mϕs (**Fig. 5*A***). The amounts of AA released in M-CSF Mϕs were 2–3% of total AA, according to a recent fatty acid analysis of similar cells (27). On the other hand, in incubations with ionophore together with exogenous AA, formation of 5-HETE was highest in GM-CSF cells, which corresponded to the 5-LO protein expression (Fig. 5*B*). A possible reason for this discrepancy is the more efficient release of endogenous AA in incubations of M-CSF cells with the bacterial stimuli. In human neutrophils, LPS/fMLP stimulation is known to activate $cPLA_2$ by increased phosphorylation (28). We found an increased P-$cPLA_2$ Western blot band also in human Mϕs, particularly for M-CSF Mϕs in response to LPS/fMLP and PGN (Fig. 5*C*, *D*). In these cells the basal P-$cPLA_2$/$cPLA_2$ ratio was low but increased considerably upon stimulation. On the other hand, for GM-CSF Mϕs the basal P-$cPLA_2$/$cPLA_2$ ratio was high

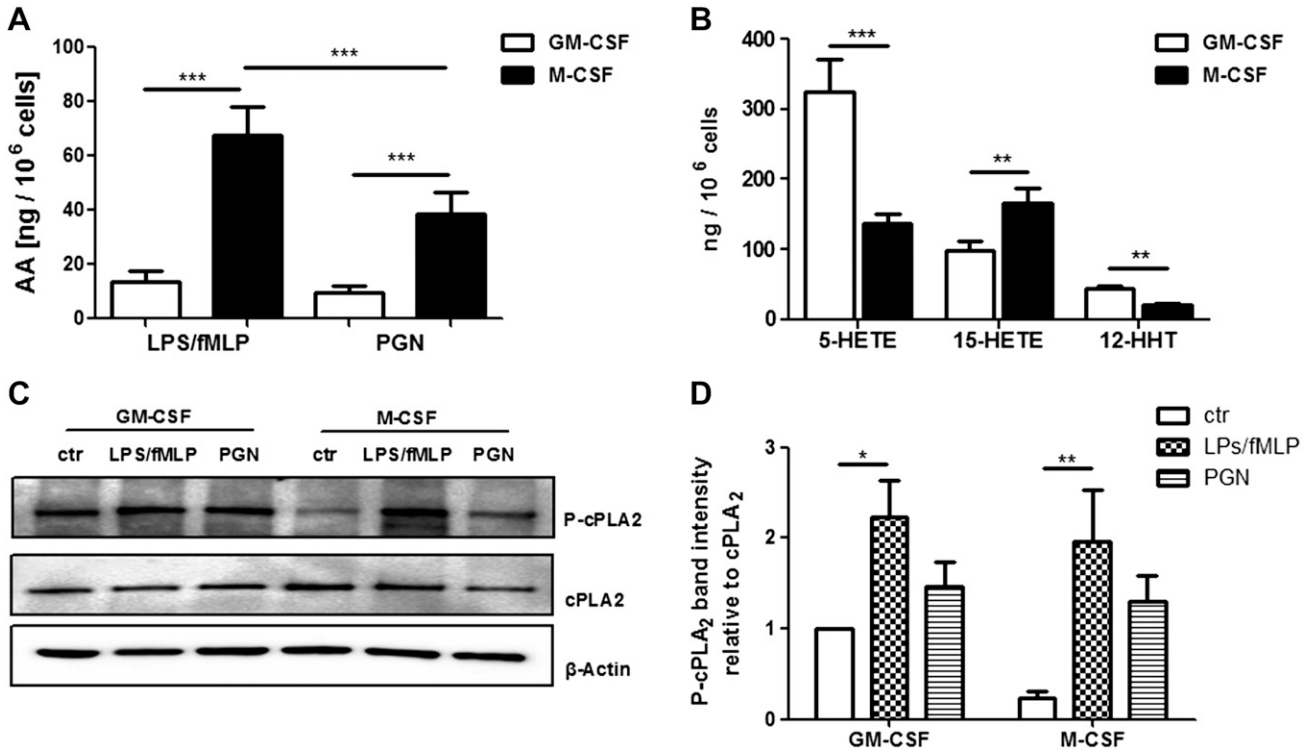

Figure 5. Bacterial stimuli activate $cPLA_2$ more efficiently in M-CSF Mϕs. *A*) Release of AA in GM-CSF and M-CSF Mϕs in response to bacterial stimuli. Data are from the lipidomic analyses described in Fig. 3 and Supplemental Table 1. *B*) Formation of HETEs from exogenous substrate. GM-CSF– and M-CSF–differentiated Mϕs were incubated with exogenous AA (40 μM) together with ionophore A23187 (5 μM) for 10 min. Samples were extracted and analyzed by HPLC with UV detection. Data are presented as means ± SE of cells from 5 donors and 2 incubations for each cell type ($n = 10$). *C*, *D*) Phosphorylation of $cPLA_2$ in GM-CSF– and M-CSF–differentiated Mϕs stimulated with LPS (1 μg/ml) for 20 min plus fMLP (1 μM) for 10 min or with peptidoglycan (100 μg/ml) for 30 min. *C*) Cell lysates (40 μg protein; see Materials and Methods) were analyzed by SDS-PAGE and Western blots for $cPLA_2$ and P-$cPLA_2$. Similar results were observed for 3 additional donors. *D*) Band intensity ratios (P-$cPLA_2$/$cPLA_2$) for control and cells subjected to bacterial stimuli. The ratio for GM-CSF control cells was set as 1, and the other ratios were normalized to GM-CSF control. Data are presented as means ± SE ($n = 4$). $^*P < 0.05$, $^{**}P < 0.01$, $^{***}P < 0.001$.

and increased only modestly upon stimulation. These results suggest that exposure of M-CSF Mϕs to bacterial stimuli induced a more prominent acute increase in $cPLA_2$ activity as compared with GM-CSF cells.

In incubations with ionophore A23187 and exogenous AA, also formation of 15-HETE was greatly increased (~1000-fold) compared with the bacterial stimuli, which gave only small amounts of 15-HETE (Fig. 5*B*). Thus, 15-LO, which is abundant in M-CSF Mϕs (Fig. 4), was active. This suggests that the endogenous AA released from cellular phospholipids in response to bacterial stimuli was available primarily for 5-LO and COX1 pathways and not for 15-LO. In the incubations with ionophore A23187 and exogenous AA, the highest amounts of 5-HETE were produced in the GM-CSF cells (~100-fold more compared with incubations with LPS/fMLP). When cells are incubated with A23187 plus exogenous AA, physiologic regulation of enzyme activities is largely bypassed, and product formation primarily reflects the amounts of enzymes.

Activation of 5-LO in cells includes translocation of 5-LO to the nuclear membrane (29). To investigate this, we performed Western blot of cytosolic and nuclear fractions and immunocytochemistry as described by Lukic *et al.* (18). Stimulation of both Mϕ types with LPS/fMLP increased the association of 5-LO with the nuclear fraction (Supplemental Fig. 2*A*, *B*). However, the change was not very striking, which may be related to the high relative amount of 5-LO localized in the nucleus of resting cells. Immunocytochemistry showed that 5-LO was present in the cytosol and inside the nuclei of GM-CSF and M-CSF cells (Supplemental Fig. 2*C*). Overall staining was more intense in GM-CSF cells, in agreement with the Western blot results. When cells were stimulated with ionophore, perinuclear rings appeared for both cell types, but this was not clearly observed with the bacterial stimuli.

DISCUSSION

The time course of inflammation can be described as a sequence of overlapping phases, starting with initiation and ending with resolution (30). Within this sequence of events, different types of Mϕs are active (2). First, tissue Mϕs, with intrinsic anti-inflammatory properties, take part in sensing alarm signals. These signals and mediators produced by the activated tissue Mϕs lead to recruitment of monocytes and differentiation of these to M1 phenotypes. When the alarm signal subsides, this is followed by the appearance of anti-inflammatory and healing Mϕs, leading to restoration of tissue homeostasis. Lipid mediators are involved in all phases of inflammation, from initiation to resolution (31).

Colony-stimulating factors are fundamental for the development and differentiation of Mϕs (32). M-CSF expressed constitutively in the steady state confers differentiation to normal resident Mϕs, whereas GM-CSF increased during inflammation leads to proinflammatory M1 Mϕs (32). We differentiated human monocytes with GM-CSF or M-CSF, which are known to prime toward M1 or M2 phenotypes, respectively (15). Eicosanoid formation in these cells was analyzed by LC-MS/MS in 2 types of samples. Basal release of lipid mediators was determined by extraction of the conditioned cell culture medium (final 24 h of the differentiation). Induced formation of eicosanoids was determined by incubating the differentiated washed Mϕs with bacterial stimuli.

In the absence of stimulation during ordinary cell culture, the major eicosanoids released were LXA_4 and PGE_2. The levels for LXA_4 were quite similar to previous findings for fully activated endpoint M1/M2 Mϕs (14). Lipoxin biosynthesis typically involves transcellular metabolism (7), but LXA_4 can also be formed within Mϕs (8), as confirmed here. Mϕs are well-known producers of PGE_2, and this can be up-regulated by LPS and zymosan (33, 34). It is of interest that we found the PGE_2 metabolite tetranor-PGEM rather than PGE_2. Mϕs express 15-hydroxyprostaglandin dehydrogenase (35) and genes for mitochondrial β-oxidation (36, 37); thus, it appears reasonable that tetranor-PGEM could be formed over time in these cell cultures. Also, TxB_2 was abundant in the conditioned media from both Mϕ types. TxA_2 is often described as proinflammatory (*e.g.*, in muscarinic acetylcholine receptor–mediated airway constriction) (38). However, TxA_2-TP signaling also modulated immunity to foreign antigens by negatively regulating dendritic cell–T cell interactions (39). Apparently, thromboxane formation in monocytic cells may have both pro- and anti-inflammatory effects. An interesting EPA metabolite in the Mϕ-conditioned medium was 18-HEPE, an intermediate in RvE formation (Fig. 2*J*) (20). M2 Mϕs release 2-fold more RvE2 in comparison to M1 (14); the similar trend in the metabolism of the RvE2 precursor 18-HEPE by M-CSF cells suggests that priming for increased RvE formation may occur early during Mϕ differentiation prior to full M2 activation. More recently, it was also found that Mϕ-derived 18-HEPE could prevent pressure overload–induced cardiac remodeling (40).

When the same Mϕs were incubated with bacterial stimuli (30 min, LPS/fMLP or PGN), both cell types produced LTB_4 and TxB_2 in similar amounts. A striking difference was that the M-CSF Mϕs produced high amounts of LTC_4. This is of considerable interest in relation to the role of Cys-LTs in T-helper 2–driven asthma, in which there is an enhanced presence of M2 Mϕs (22, 41). Cys-LTs are very potent inducers of vascular permeability in postcapillary venules, leading to exudates containing plasma proteins including the complement system, which can opsonize all bacteria and can lyse Gram-negative bacteria. As demonstrated in the zymosan-induced peritonitis model (42, 43), this early event in acute inflammation can be induced by resident peritoneal Mϕs present at the site of infection or injury *via* prompt formation of Cys-LTs. It has been emphasized that M-CSF promotes viability and proliferation of tissue-resident Mϕs of M2 character (15). It appears possible that the M-CSF cells studied here may bear traits resembling resident Mϕs.

Mϕ in the M2 spectrum confer fibrosis and remodeling (22, 41), and another effect of Cys-LTs is induction of TGF-β, furin, and VEGF, leading to tissue remodeling in chronic asthma (44–46). It is tempting to speculate that the M-CSF–derived Mϕs studied here, with high capacity for

LTC_4 biosynthesis, may resemble pulmonary M2 cells active in allergic lung inflammation (22). Further conversion to LTD_4 was low in the M-CSF and GM-CSF Mϕs. As discussed by Lukic *et al*. (18), epithelial cells in the lung can metabolize Mϕ-derived LTC_4 to LTD_4, leading to CysLT1-mediated effects, including tissue remodeling. Different LTC_4 synthesis capacities for different types of Mϕs have been described before. High LTC_4 biosynthesis was observed for resident mouse peritoneal Mϕs, which produced about 3-fold more LTC_4 compared with thioglycolate-elicited cells (9). A subset of Mϕs fluorescence-activated cell sorted from mouse lung tumors (MacA, representing resident alveolar Mϕs) produced LTC_4 (13). Also, these observations indicate that high LTC_4 synthesis capacity can be a characteristic for resident Mϕs of M2 character.

Thus, in resting conditions both the GM-CSF– and the M-CSF–differentiated Mϕs produced primarily anti-inflammatory and proresolving lipid mediators, but when encountering bacterial stimuli the same cells quickly switched to production of proinflammatory LTs. During these 30-min incubations with bacterial stimuli, the short time span should preclude a change of cell phenotype along the M1/M2 spectrum. The prompt change to proinflammatory mediator formation seems rather to be a possibility characterizing eicosanoid biosynthesis, exploited by both Mϕ types. In comparison, when Mϕs up- or down-regulate formation of pro- or anti-inflammatory cytokines, this appears to be connected with more long-term changes of Mϕ phenotype (4, 22).

When M-CSF Mϕs were incubated with the bacterial stimuli, they showed a high capacity to mobilize AA from phospholipids. Interestingly, CD14, which was 3–4 times more abundant on M-CSF Mϕs (Fig. 1), is involved in both TLR4 and TLR2 signaling (19). This could be related to the activation the $cPLA_2$ and higher AA release in M-CSF cells. Translocation of 5-LO to the nuclear membrane determines LT biosynthesis (29). In these Mϕs, most 5-LO was found in the nuclear fraction already in resting cells, compatible with previously described intranuclear localization (47). LPS/fMLP (but not peptidoglycan) increased nuclear association about 2-fold in both cell types. When stimulated with ionophore perinuclear rings could be observed, but not so with the bacterial stimuli. These observations may indicate that a minor part of 5-LO translocated to the nuclear membrane or that 5-LO could be active inside the nucleus; no difference between the 2 Mϕ types could be observed. Other possible mechanisms for the high formation of LTC_4 and 5-HETE in M-CSF cells may be related to the phosphorylation status of 5-LO and LTC_4 synthase, formation of LTC_4 synthase–FLAP complexes, and the expression level of CLP (higher in M-CSF cells). Interestingly, RvD1 was found to limit nuclear localization of 5-LO in Mϕs *via* inhibition of calmodulin-dependent protein kinase II (48). As reviewed by Dennis and Norris (6), the availability of endogenous AA to the different COX and LOX enzymes and assembly of enzyme systems may also apply. Expression of 15-LOX-1 was higher in M-CSF Mϕs as compared with GM-CSF cells (Fig. 4). IL-4 is well known to up-regulate 15-LOX-1 (49), and this has been included as a criterion for M2 differentiation (3). Apparently, initiation of Mϕ polarization in M2 direction by M-CSF is sufficient to up-regulate 15-LOX-1, thus increasing the capacity for formation of lipoxins and resolvins.

In addition to Mϕ subtype-specific differences in oxylipin biosynthesis, a few reports on the induction of Mϕ polarization by lipid mediators have appeared. Human M1 Mϕs were incubated with 13S,14S-epoxy-maresin, which down-regulated CD54 and CD80 and up-regulated CD163 and CD206, indicating a change toward the M2 phenotype (50). Differentiation of alternatively activated Mϕs in respiratory syncytial virus infection involved LOX pathways (LXA_4 and RvE_1) (51). For mouse peritoneal Mϕs, EpETrEs (particularly 11,12-EpETrE) regulated polarization by attenuating NF-κB *via* activation of peroxisome proliferator-activated receptor-α/γ and heme oxygenase 1 (52). *Via* cAMP/cAMP response element binding protein, PGE_2 enhanced M2 polarization of mouse bone marrow–derived Mϕs (53). PGE_2 also induced IL-10–producing Mϕs *in vitro* and reduced allergic lung inflammation in mice (54).

In summary, resting Mϕs released mainly anti-inflammatory lipid mediators but promptly shifted toward inflammatory lipid metabolism upon bacterial stimulation. The main differences in their metabolism and protein expression partially reflected possible associations with M1/M2 functions. There are still several discrepancies in the M1/M2 field. One possible reason may be the initial CSF used in differentiation protocols. Our results suggest that the efficiency of GM-CSF and M-CSF to drive Mϕs toward M1/M2 phenotypes includes priming effects on eicosanoid biosynthesis, which can affect the final shift toward inflammatory or resolving functions. FJ

ACKNOWLEDGMENTS

The authors thank Johan Kolmert (Department of Environmental Medicine, Karolinska Institutet) for kind help and discussions. This work was supported by grants from the Swedish Medical Research Council, the Swedish Cancer Foundation, the Cancer Research Foundations of Radiumhemmet, the Stockholm County Council, the Swedish Heart-Lung Foundation, the Center for Allergy Research, the Cancer and Allergy Foundation, the AstraZeneca Joint Research Program in Translational Science (ChAMP), and the Hesselman Foundation, and from the Karolinska Institute (all in Stockholm, Sweden). A.F. was funded by the Karin and Sten Mörtstedt Initiative on Anaphylaxis (Stockholm, Sweden). C.E.W. was supported by the Swedish Heart Lung Foundation (HLF 20150640). The authors declare no conflicts of interest.

AUTHOR CONTRIBUTIONS

A. Lukic and O. Radmark conceived the research plan; A. Lukic, P. Larssen, and A. Fauland designed and performed the experiments; A. Lukic analyzed the data; A. Lukic and O. Radmark wrote the manuscript; and all authors revised and contributed to the manuscript.

REFERENCES

1. Soehnlein, O., and Lindbom, L. (2010) Phagocyte partnership during the onset and resolution of inflammation. *Nat. Rev. Immunol.* **10**, 427–439

2. Murray, P. J., and Wynn, T. A. (2011) Protective and pathogenic functions of macrophage subsets. *Nat. Rev. Immunol.* **11**, 723–737
3. Murray, P. J., Allen, J. E., Biswas, S. K., Fisher, E. A., Gilroy, D. W., Goerdt, S., Gordon, S., Hamilton, J. A., Ivashkiv, L. B., Lawrence, T., Locati, M., Mantovani, A., Martinez, F. O., Mege, J. L., Mosser, D. M., Natoli, G., Saeij, J. P., Schultze, J. L., Shirey, K. A., Sica, A., Suttles, J., Udalova, I., van Ginderachter, J. A., Vogel, S. N., and Wynn, T. A. (2014) Macrophage activation and polarization: nomenclature and experimental guidelines. *Immunity* **41**, 14–20
4. Martinez, F. O., and Gordon, S. (2014) The M1 and M2 paradigm of macrophage activation: time for reassessment. *F1000Prime Rep.* **6**, 13
5. Martinez, F. O., Gordon, S., Locati, M., and Mantovani, A. (2006) Transcriptional profiling of the human monocyte-to-macrophage differentiation and polarization: new molecules and patterns of gene expression. *J. Immunol.* **177**, 7303–7311
6. Dennis, E. A., and Norris, P. C. (2015) Eicosanoid storm in infection and inflammation. *Nat. Rev. Immunol.* **15**, 511–523
7. Serhan, C. N. (2002) Lipoxins and aspirin-triggered 15-epi-lipoxin biosynthesis: an update and role in anti-inflammation and pro-resolution. *Prostaglandins Other Lipid Mediat.* **68–69**, 433–455
8. Norris, P. C., Gosselin, D., Reichart, D., Glass, C. K., and Dennis, E. A. (2014) Phospholipase A2 regulates eicosanoid class switching during inflammasome activation. *Proc. Natl. Acad. Sci. USA* **111**, 12746–12751
9. Kita, Y., Takahashi, T., Uozumi, N., Nallan, L., Gelb, M. H., and Shimizu, T. (2005) Pathway-oriented profiling of lipid mediators in macrophages. *Biochem. Biophys. Res. Commun.* **330**, 898–906
10. Buczynski, M. W., Stephens, D. L., Bowers-Gentry, R. C., Grkovich, A., Deems, R. A., and Dennis, E. A. (2007) TLR-4 and sustained calcium agonists synergistically produce eicosanoids independent of protein synthesis in RAW264.7 cells. *J. Biol. Chem.* **282**, 22834–22847
11. Norris, P. C., and Dennis, E. A. (2012) Omega-3 fatty acids cause dramatic changes in TLR4 and purinergic eicosanoid signaling. *Proc. Natl. Acad. Sci. USA* **109**, 8517–8522
12. Lundström, S. L., Saluja, R., Adner, M., Haeggström, J. Z., Nilsson, G., and Wheelock, C. E. (2013) Lipid mediator metabolic profiling demonstrates differences in eicosanoid patterns in two phenotypically distinct mast cell populations. *J. Lipid Res.* **54**, 116–126
13. Poczobutt, J. M., Gijon, M., Amin, J., Hanson, D., Li, H., Walker, D., Weiser-Evans, M., Lu, X., Murphy, R. C., and Nemenoff, R. A. (2013) Eicosanoid profiling in an orthotopic model of lung cancer progression by mass spectrometry demonstrates selective production of leukotrienes by inflammatory cells of the microenvironment. *PLoS One* **8**, e79633
14. Dalli, J., and Serhan, C. N. (2012) Specific lipid mediator signatures of human phagocytes: microparticles stimulate macrophage efferocytosis and pro-resolving mediators. *Blood* **120**, e60–e72
15. Hamilton, T. A., Zhao, C., Pavicic, P. G., Jr., and Datta, S. (2014) Myeloid colony-stimulating factors as regulators of macrophage polarization. *Front. Immunol.* **5**, 554
16. Esser, J., U. Gehrmann, F. L. D'Alexandri, A. M. Hidalgo-Estevez, C. E. Wheelock, A. Scheynius, S. Gabrielsson, and O. Radmark. (2010). Exosomes from human macrophages and dendritic cells contain enzymes for leukotriene biosynthesis and promote granulocyte migration. *J. Allergy Clin. Immunol.* **126**, 1032–1040, 1040.e1-4.
17. Balgoma, D., Yang, M., Sjödin, M., Snowden, S., Karimi, R., Levänen, B., Merikallio, H., Kaarteenaho, R., Palmberg, L., Larsson, K., Erle, D. J., Dahlén, S. E., Dahlén, B., Sköld, C. M., Wheelock, A. M., and Wheelock, C. E. (2016) Linoleic acid-derived lipid mediators increase in a female-dominated subphenotype of COPD. *Eur. Respir. J.* **47**, 1645–1656
18. Lukic, A., Ji, J., Idborg, H., Samuelsson, B., Palmberg, L., Gabrielsson, S., and Rådmark, O. (2016) Pulmonary epithelial cancer cells and their exosomes metabolize myeloid cell-derived leukotriene C4 to leukotriene D4. *J. Lipid Res.* **57**, 1659–1669
19. Dziarski, R. (2003) Recognition of bacterial peptidoglycan by the innate immune system. *Cell. Mol. Life Sci.* **60**, 1793–1804
20. Tjonahen, E., Oh, S. F., Siegelman, J., Elangovan, S., Percarpio, K. B., Hong, S., Arita, M., and Serhan, C. N. (2006) Resolvin E2: identification and anti-inflammatory actions: pivotal role of human 5-lipoxygenase in resolvin E series biosynthesis. *Chem. Biol.* **13**, 1193–1202
21. Zhang, Y., Guallar, E., Blasco-Colmenares, E., Harms, A. C., Vreeken, R. J., Hankemeier, T., Tomaselli, G. F., and Cheng, A. (2016) Serum-based oxylipins are associated with outcomes in primary prevention implantable cardioverter defibrillator patients. *PLoS One* **11**, e0157035
22. Jiang, Z., and Zhu, L. (2016) Update on the role of alternatively activated macrophages in asthma. *J. Asthma Allergy* **9**, 101–107
23. Lehmann, C., Homann, J., Ball, A. K., Blöcher, R., Kleinschmidt, T. K., Basavarajappa, D., Angioni, C., Ferreirós, N., Häfner, A. K., Rådmark, O., Proschak, E., Haeggström, J. Z., Geisslinger, G., Parnham, M. J., Steinhilber, D., and Kahnt, A. S. (2015) Lipoxin and resolvin biosynthesis is dependent on 5-lipoxygenase activating protein. *FASEB J.* **29**, 5029–5043
24. Sokolowska, M., Chen, L. Y., Eberlein, M., Martinez-Anton, A., Liu, Y., Alsaaty, S., Qi, H. Y., Logun, C., Horton, M., and Shelhamer, J. H. (2014) Low molecular weight hyaluronan activates cytosolic phospholipase A2α and eicosanoid production in monocytes and macrophages. *J. Biol. Chem.* **289**, 4470–4488
25. Haeggström, J. Z., and Funk, C. D. (2011) Lipoxygenase and leukotriene pathways: biochemistry, biology, and roles in disease. *Chem. Rev.* **111**, 5866–5898
26. Mandal, A. K., Jones, P. B., Bair, A. M., Christmas, P., Miller, D., Yamin, T. T., Wisniewski, D., Menke, J., Evans, J. F., Hyman, B. T., Bacskai, B., Chen, M., Lee, D. M., Nikolic, B., and Soberman, R. J. (2008) The nuclear membrane organization of leukotriene synthesis. *Proc. Natl. Acad. Sci. USA* **105**, 20434–20439
27. Varin, A., Thomas, C., Ishibashi, M., Ménégaut, L., Gautier, T., Trousson, A., Bergas, V., de Barros, J. P., Narce, M., Lobaccaro, J. M., Lagrost, L., and Masson, D. (2015) Liver X receptor activation promotes polyunsaturated fatty acid synthesis in macrophages: relevance in the context of atherosclerosis. *Arterioscler. Thromb. Vasc. Biol.* **35**, 1357–1365
28. Surette, M. E., Dallaire, N., Jean, N., Picard, S., and Borgeat, P. (1998) Mechanisms of the priming effect of lipopolysaccharides on the biosynthesis of leukotriene B4 in chemotactic peptide-stimulated human neutrophils. *FASEB J.* **12**, 1521–1531
29. Rådmark, O., Werz, O., Steinhilber, D., and Samuelsson, B. (2015) 5-Lipoxygenase, a key enzyme for leukotriene biosynthesis in health and disease. *Biochim. Biophys. Acta* **1851**, 331–339
30. Lawrence, T., Willoughby, D. A., and Gilroy, D. W. (2002) Anti-inflammatory lipid mediators and insights into the resolution of inflammation. *Nat. Rev. Immunol.* **2**, 787–795
31. Serhan, C. N. (2017) Treating inflammation and infection in the 21st century: new hints from decoding resolution mediators and mechanisms. *FASEB J.* **31**, 1273–1288
32. Hamilton, J. A. (2008) Colony-stimulating factors in inflammation and autoimmunity. *Nat. Rev. Immunol.* **8**, 533–544
33. Fu, J. Y., Masferrer, J. L., Seibert, K., Raz, A., and Needleman, P. (1990) The induction and suppression of prostaglandin H2 synthase (cyclooxygenase) in human monocytes. *J. Biol. Chem.* **265**, 16737–16740
34. Esser, J., Gehrmann, U., Salvado, M. D., Wetterholm, A., Haeggström, J. Z., Samuelsson, B., Gabrielsson, S., Scheynius, A., and Rådmark, O. (2011) Zymosan suppresses leukotriene C_4 synthase activity in differentiating monocytes: antagonism by aspirin and protein kinase inhibitors. *FASEB J.* **25**, 1417–1427
35. Wei, C., Zhu, P., Shah, S. J., and Blair, I. A. (2009) 15-oxo-eicosatetraenoic acid, a metabolite of macrophage 15-hydroxyprostaglandin dehydrogenase that inhibits endothelial cell proliferation. *Mol. Pharmacol.* **76**, 516–525
36. Cabrero, A., Cubero, M., Llaverías, G., Jové, M., Planavila, A., Alegret, M., Sánchez, R., Laguna, J. C., and Carrera, M. V. (2003) Differential effects of peroxisome proliferator-activated receptor activators on the mRNA levels of genes involved in lipid metabolism in primary human monocyte-derived macrophages. *Metabolism* **52**, 652–657
37. Namgaladze, D., and Brüne, B. (2014) Fatty acid oxidation is dispensable for human macrophage IL-4-induced polarization. *Biochim. Biophys. Acta* **1841**, 1329–1335
38. Allen, I. C., Hartney, J. M., Coffman, T. M., Penn, R. B., Wess, J., and Koller, B. H. (2006) Thromboxane A2 induces airway constriction through an M3 muscarinic acetylcholine receptor-dependent mechanism. *Am. J. Physiol. Lung Cell. Mol. Physiol.* **290**, L526–L533
39. Matsuoka, T., and Narumiya, S. (2007) Prostaglandin receptor signaling in disease. *Sci. World J.* **7**, 1329–1347
40. Endo, J., Sano, M., Isobe, Y., Fukuda, K., Kang, J. X., Arai, H., and Arita, M. (2014) 18-HEPE, an n-3 fatty acid metabolite released by macrophages, prevents pressure overload-induced maladaptive cardiac remodeling. *J. Exp. Med.* **211**, 1673–1687
41. Moreira, A. P., and Hogaboam, C. M. (2011) Macrophages in allergic asthma: fine-tuning their pro- and anti-inflammatory actions for disease resolution. *J. Interferon Cytokine Res.* **31**, 485–491

42. Kolaczkowska, E., Shahzidi, S., Seljelid, R., van Rooijen, N., and Plytycz, B. (2002) Early vascular permeability in murine experimental peritonitis is co-mediated by resident peritoneal macrophages and mast cells: crucial involvement of macrophage-derived cysteinyl-leukotrienes. *Inflammation* **26**, 61–71
43. Rossi, A., Pergola, C., Pace, S., Rådmark, O., Werz, O., and Sautebin, L. (2014) In vivo sex differences in leukotriene biosynthesis in zymosan-induced peritonitis. *Pharmacol. Res.* **87**, 1–7
44. Bossé, Y., Thompson, C., McMahon, S., Dubois, C. M., Stankova, J., and Rola-Pleszczynski, M. (2008) Leukotriene D4-induced, epithelial cell-derived transforming growth factor beta1 in human bronchial smooth muscle cell proliferation. *Clin. Exp. Allergy* **38**, 113–121
45. Thompson, C., McMahon, S., Bossé, Y., Dubois, C. M., Stankova, J., and Rola-Pleszczynski, M. (2008) Leukotriene D4 up-regulates furin expression through CysLT1 receptor signaling. *Am. J. Respir. Cell Mol. Biol.* **39**, 227–234
46. Poulin, S., Thompson, C., Thivierge, M., Véronneau, S., McMahon, S., Dubois, C. M., Stankova, J., and Rola-Pleszczynski, M. (2011) Cysteinyl-leukotrienes induce vascular endothelial growth factor production in human monocytes and bronchial smooth muscle cells. *Clin. Exp. Allergy* **41**, 204–217
47. Werz, O. (2002) 5-lipoxygenase: cellular biology and molecular pharmacology. *Curr. Drug Targets Inflamm. Allergy* **1**, 23–44
48. Fredman, G., Ozcan, L., Spolitu, S., Hellmann, J., Spite, M., Backs, J., and Tabas, I. (2014) Resolvin D1 limits 5-lipoxygenase nuclear localization and leukotriene B4 synthesis by inhibiting a calcium-activated kinase pathway. *Proc. Natl. Acad. Sci. USA* **111**, 14530–14535
49. Ivanov, I., Kuhn, H., and Heydeck, D. (2015) Structural and functional biology of arachidonic acid 15-lipoxygenase-1 (ALOX15). *Gene* **573**, 1–32
50. Dalli, J., Zhu, M., Vlasenko, N. A., Deng, B., Haeggström, J. Z., Petasis, N. A., and Serhan, C. N. (2013) The novel 13S,14S-epoxy-maresin is converted by human macrophages to maresin 1 (MaR1), inhibits leukotriene A4 hydrolase (LTA4H), and shifts macrophage phenotype. *FASEB J.* **27**, 2573–2583
51. Shirey, K. A., Lai, W., Pletneva, L. M., Karp, C. L., Divanovic, S., Blanco, J. C., and Vogel, S. N. (2014) Role of the lipoxygenase pathway in RSV-induced alternatively activated macrophages leading to resolution of lung pathology. *Mucosal Immunol.* **7**, 549–557
52. Dai, M., Wu, L., He, Z., Zhang, S., Chen, C., Xu, X., Wang, P., Gruzdev, A., Zeldin, D. C., and Wang, D. W. (2015) Epoxyeicosatrienoic acids regulate macrophage polarization and prevent LPS-induced cardiac dysfunction. *J. Cell. Physiol.* **230**, 2108–2119
53. Luan, B., Yoon, Y. S., Le Lay, J., Kaestner, K. H., Hedrick, S., and Montminy, M. (2015) CREB pathway links PGE2 signaling with macrophage polarization. *Proc. Natl. Acad. Sci. USA* **112**, 15642–15647
54. Draijer, C., Boorsma, C. E., Reker-Smit, C., Post, E., Poelstra, K., and Melgert, B. N. (2016) PGE2-treated macrophages inhibit development of allergic lung inflammation in mice. *J. Leukoc. Biol.* **100**, 95–102

Received for publication April 10, 2017.
Accepted for publication May 30, 2017.